

Sunspot Time Series: Passive and Active Intervals

S. Zięba · Z. Nieckarz

Received: 26 September 2013 / Accepted: 7 February 2014 / Published online: 26 February 2014
© The Author(s) 2014. This article is published with open access at Springerlink.com

Abstract Solar activity slowly and irregularly decreases from the first spotless day (FSD) in the declining phase of the old sunspot cycle and systematically, but also in an irregular way, increases to the new cycle maximum after the last spotless day (LSD). The time interval between the first and the last spotless day can be called the passive interval (PI), while the time interval from the last spotless day to the first one after the new cycle maximum is the related active interval (AI). Minima of solar cycles are inside PIs, while maxima are inside AIs. In this article, we study the properties of passive and active intervals to determine the relation between them. We have found that some properties of PIs, and related AIs, differ significantly between two group of solar cycles; this has allowed us to classify Cycles 8–15 as passive cycles, and Cycles 17–23 as active ones. We conclude that the solar activity in the PI declining phase (a descending phase of the previous cycle) determines the strength of the approaching maximum in the case of active cycles, while the activity of the PI rising phase (a phase of the ongoing cycle early growth) determines the strength of passive cycles. This can have implications for solar dynamo models. Our approach indicates the important role of solar activity during the declining and the rising phases of the solar-cycle minimum.

Keywords Spotless days · Solar phase tracking · Waldmeier effect · Prediction

1. Introduction

In a recently published paper (Zięba and Nieckarz, 2012), we have shown that the relations based on the position of the longest spotless segment (LSS, the longest sequence of consecutive days when no spots were observed) with respect to locations of some characteristic

S. Zięba (✉)
Astronomical Observatory, Jagiellonian University, Orla 171, 30-244, Kraków, Poland
e-mail: stanzieba712@gmail.com

Z. Nieckarz
Institute of Physics, Jagiellonian University, Reymonta 4, 30-059, Kraków, Poland
e-mail: zenon.nieckarz@uj.edu.pl

extreme points in the daily sunspot numbers are statistically significant and have a predictive value. This indicates that the passive interval (PI) as well as the location and length of the LSS can be useful for studying of the physical processes responsible for the solar variability, especially since their values do not result from any smoothing procedure but are really observed.

In this article, we examine relationships between various parameters characterizing the passive and active intervals whose definition was given by Zięba *et al.* (2006). The active interval (AI) complements the passive interval in the sense that it covers also the time interval between the border spotless days but includes the cycle maximum. The proposed decomposition of sunspot time series into passive and active intervals is unambiguous. PI and related AI carry the same number, which is assigned from the number of the cycle of which minimum and maximum are inside of these intervals. Each passive interval and the active interval occurring after it form the ordered pair PI–AI. As the classically understood solar cycle and the pair PI–AI with the same number include the same maximum phase of solar cycle we use the name cycle also for the ordered pair PI–AI.

The basis for our research was and is the daily international sunspot number (ISN) series provided by the Solar Influences Data Center (SIDC, <http://sidc.oma.be/>) of the Royal Observatory of Belgium. Until 1980 the ISN, better known as the Wolf or Zürich number, was compiled by the Swiss Federal Observatory. In this work we use the daily ISN series covering the period between January 1830 and June 2012. This period includes the decline phase of Cycle 7, Cycles 8–23 and the initial rise of Cycle 24. Cycles 7–9 include the era of Schwabe's records with a large number of days without observations (Wilson, 1998). Cycles 10, 11, and the rise of Cycle 12 belong to Wolf's era (years 1848–1882), while those of Cycles 13–21 belong to the Zürich era. Since 1981, when the International Astronomical Union World Data Center for sunspot numbers was transferred from the Zürich Observatory to Brussels, a new approach for calculation of the sunspot number has been established (Clette *et al.*, 2007). The intrinsic nature and accuracy for four main eras of sunspot number observations are different in the ISN time series and this is the reason for treating the daily ISN series with care. However, we have shown in Zięba and Nieckarz (2012) that differences arising from heterogeneous ISN data among Cycles 8–23 can be neglected.

This article is organized as follows. In Section 2 we describe characteristic points of the daily ISN series and define various time intervals whose lengths and amplitudes are studied in Sections 3 and 4. Next, in Section 5 we discuss relations between lengths (periods) and amplitudes (strength) of the intervals considered, including the Waldmeier effect. Some predictions for Cycle 24 are given in Section 6, and Section 7 comprises a summary and a discussion.

2. Definition of Characteristic Points and Time Intervals

The passive interval (PI) is defined as the time interval (denoted '00') from the first spotless day (FSD) after an old cycle maximum to the last spotless day (LSD) before the next new cycle maximum (Zięba *et al.*, 2006; Zięba and Nieckarz, 2012). All spotless days occur within the passive intervals. For each passive interval we have a minimum of activity (cycle minimum) and the occurrence of the longest spotless segment (LSS). We accept the center of LSS as the distinctive point of the PI.

The idea of using spotless days to find the minimum of activity was suggested by Waldmeier (1961) and McKinnon (1987). Wilson (1995) proposed to use the first spotless day as

Table 1 Definitions of the intervals and the time distances used in this article.

Interval (distance)	Definition	Cycle		All cycle	
		14	22	Mean	sem ¹
[days]					
00 ²	Passive interval (PI), the time interval covering all the days from the first spotless day (FSD) after a cycle maximum to the last spotless day (LSD) before the next cycle maximum along with them	3548	1331	2334	216
0s	Declining segment of the PI, the time interval from the FSD after a cycle maximum to the central day of the LSS	1983	774	1512	131
s0	Rising segment of the PI, the time interval from the central day of the LSS to the LSD before the next cycle maximum	1565	557	822	100
0m	The time distance from the FSD after a cycle maximum to the day of minimum given by the 810-day Gaussian filter (Gaussian minimum, Gm)	2105	834	1404	138
0p	The time distance from the FSD after a cycle maximum to the day with the maximal daily sunspot number (peak maximum, Px) inside the next cycle maximum	3653	2829	2919	164
0g	The time distance from the FSD after a cycle maximum to the day of maximum given by the 810-day Gaussian filter (Gaussian maximum, Gx) inside the next cycle maximum	3831	2327	3020	153
sp	The time distance from the central day of the LSS to the successive Px	1671	2056	1407	74
xx	Active interval (AI), the time interval covering all the days from the LSD after a cycle minimum to the FSD before the next cycle minimum without spotless days	445	2453	1638	173
xp	The time distance from the LSD before a cycle maximum to the Px	106	1499	585	97
px	The time distance from the Px to the FSD before the next cycle minimum	339	954	1052	109
ss	The time distance between the central days of two successive LSS	4422	3927	4002	86

¹ sem, the standard error of the mean.

² Intervals '00', 'xx', and two others similar to '0m' and '0g' were considered by Wilson and Hathaway in 2005 in a NASA Technical Report. They used a smoothed (12 month moving average) monthly mean sunspot number for calculation their time parameters.

maxima. The size of this filter is similar to the 24-month Gaussian filter used when monthly averaged sunspot numbers are considered (Hathaway, Wilson, and Reichmann, 1999; Hathaway, 2010).

Differences between the position of the LSS and the Gaussian minimum as well as between the peak maximum and the Gaussian one are small. Figure 2 depicts their locations measured with respect to the FSD. The correlation coefficients between '0s' and '0m' ($r = 0.965$) as well as between '0p' and '0g' ($r = 0.949$) are very high. In Figure 2(b), Cycle 22 clearly stands out of the relation we have found; this is probably due to the presence of three almost equal peaks (see Figure 1(a)). When the relation is calculated without in-

Table 2 Dates defining positions of characteristic points for solar cycles (N stands for the solar-cycle number): the first spotless day (FSD), the central day of the longest spotless segment (LSS), the day of the Gaussian minimum (DGm), the last spotless day (LSD), the day of the peak maximum (DPx), the day of the Gaussian maximum (DGx). The numbers related to dates are enumerated from 1 January 1818. Other acronyms and abbreviations mean: nlss, the number of spotless days in the LSS, n00, the number of spotless days in the passive interval, RGm, the value of the Gaussian minimum, RPx, the maximal sunspot number of the indicated cycle (the peak maximum), RGx, the value of the Gaussian maximum, '00', the length of the passive interval, '0s', the length of the active interval, '0p', the time distance from the FSD to the LSS, '0m', the time distance from the FSD to the DGm, '0p', the time distance from the FSD to the DPx, '0g', the time distance from the FSD to the DGx.

N	FSD		LSS		Date		nlss		n00		LSD		DPx		Date		RPx		00		0s		0p				
	Date	RGm	Date	DGm	Date	Date	Date	Date	RGm	Date	Date	DGx	Date	Date	Date	Date	xx	xx	0m	0m	0g	0g					
8	4 407	5 958	24.04.1834	5 958	24.04.1834	34	397	6 379	6 379	6 379	6 992	21.02.1837	261	1 973	1 551	2 585	24.01.1830	5 742	20.09.1833	14.0	19.06.1835	7 054	24.04.1837	127.2	1 791	1 335	2 647
9	8 141	9 661	13.06.1844	9 661	13.06.1844	21	402	10 777	10 777	10 777	10 820	16.08.1847	254	2 637	1 520	2 679	15.04.1840	9 357	14.08.1843	16.7	04.07.1847	11 136	27.06.1848	113.2	678	1 216	2 995
10	11 456	13 764	07.09.1855	13 764	07.09.1855	49	655	14 705	14 705	14 705	15 520	28.06.1860	220	3 250	2 308	4 064	13.05.1849	13 899	20.01.1856	7.9	05.04.1858	15 434	03.04.1860	90.7	1 281	2 443	3 978
11	15 987	17 914	17.01.1867	17 914	17.01.1867	38	406	18 823	18 823	18 823	19 231	26.08.1870	317	2 837	1 927	3 244	08.10.1861	17 913	16.01.1867	13.8	14.07.1869	19 348	21.12.1870	119.2	1 404	1 926	3 361
12	20 228	22 354	15.03.1879	22 354	15.03.1879	54	1 028	24 009	24 009	24 009	24 116	10.01.1884	166	3 782	2 126	3 888	19.05.1873	22 125	29.07.1878	6.3	25.09.1883	24 054	09.11.1883	63.9	473	1 897	3 826
13	24 483	26 266	29.11.1889	26 266	29.11.1889	26	736	27 014	27 014	27 014	27 616	10.08.1893	237	2 532	1 783	3 133	11.01.1885	26 064	11.05.1889	6.6	17.12.1891	27 674	07.10.1893	80.5	1 423	1 581	3 191
14	28 438	30 420	15.04.1901	30 420	15.04.1901	69	934	31 985	31 985	31 985	32 091	08.05.1906	182	3 548	1 982	3 653	10.11.1895	30 542	15.08.1901	5.0	28.07.1905	32 269	08.05.1906	59.2	445	2 104	3 831
15	32 431	34 842	24.05.1913	34 842	24.05.1913	92	1 023	36 069	36 069	36 069	36 378	07.08.1917	268	3 639	2 411	3 947	17.10.1906	34 665	28.11.1912	3.2	02.10.1916	36 507	14.12.1917	86.8	1 284	2 234	4 076
16	37 354	38 741	26.01.1924	38 741	26.01.1924	39	534	39 645	39 645	39 645	39 847	05.02.1927	173	2 292	1 387	2 493	09.04.1920	38 492	22.05.1923	10.0	18.07.1926	40 159	14.12.1927	71.1	1 522	1 138	2 805

Table 2 (Continued)

N	FSD	LSS	Date	n _{lss}	n ₀₀	LSD	DPx	Date	RPx	00	0s	Op
	Date	DGm	Date	RGm	Date	DGx	Date	RGx	xx	0m	0g	
17	41 168	42 330	23.11.1933	36	538	42 943	43 494	30.01.1937	233	1 776	1 162	2 326
	18.09.1930	42 214	30.07.1933	8.0	8.0	29.07.1935	43 828	30.12.1937	107.1	2 292	1 046	2 660
18	45 236	46 147	06.05.1944	36	269	46 644	47 261	25.05.1947	323	1 409	911	2 025
	07.11.1941	46 023	03.01.1944	15.0	15.0	15.09.1945	47 570	29.03.1948	140.5	1 921	787	2 334
19	48 566	49 842	18.06.1954	30	446	50 329	51 127	24.12.1957	355	1 764	1 276	2 561
	20.12.1950	49 704	31.01.1954	12.8	12.8	18.10.1955	51 180	15.02.1958	185.8	2 205	1 138	2 614
20	52 535	53 591	22.09.1964	15	227	54 278	55 207	24.02.1969	215	1 744	1 056	2 672
	01.11.1961	53 602	03.10.1964	16.2	16.2	10.08.1966	55 227	16.03.1969	106.0	2 538	1 067	2 692
21	56 817	57 910	20.07.1976	24	272	58 273	59 118	10.11.1979	302	1 457	1 093	2 301
	23.07.1973	57 766	27.02.1976	16.8	16.8	18.07.1977	59 321	31.05.1980	150.4	2 317	949	2 504
22	60 591	61 364	03.01.1986	21	273	61 921	63 420	21.08.1991	300	1 331	773	2 829
	22.11.1983	61 424	04.03.1986	17.5	17.5	14.07.1987	62 918	06.04.1990	148.3	2 453	833	2 327
23	64 375	65 291	04.10.1996	42	309	65 753	66 675	19.07.2000	246	1 379	916	2 300
	02.04.1994	65 129	25.04.1996	13.4	13.4	09.01.1998	66 853	13.01.2001	112.4	2 208	754	2 478
24	67 962	69 991	17.08.2009	32	817	70 718	?	?	?	2 757	2 029	?
	27.01.2004	69 656	16.09.2008	4.0	4.0	14.08.2011	?	?	?	?	1 694	?

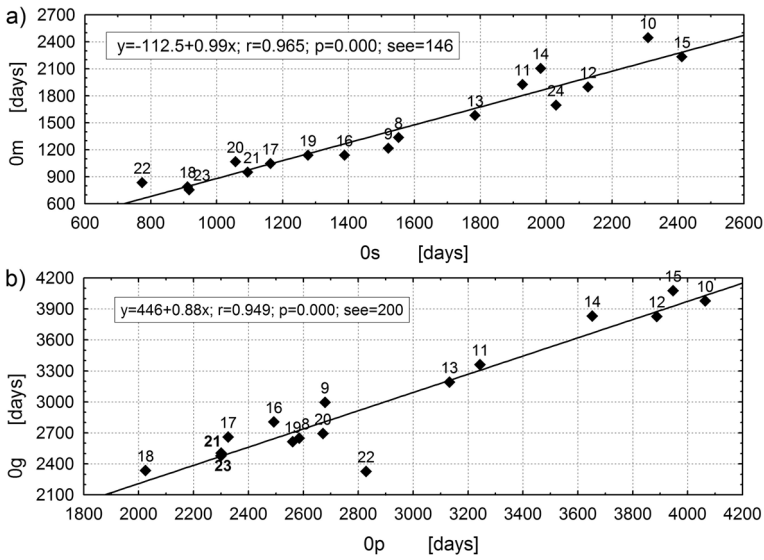


Figure 2 (a) Scatterplot of time distances ‘Om’ (positions of the Gaussian minimum) versus ‘Os’ (positions of the LSS). (b) Similar to (a) for ‘Og’ (positions of the Gaussian maximum) versus ‘Op’ (positions of the peak maximum) for the indicated cycles. The equation of the best linear fit, the correlation coefficient (r), the significance level (p), and the standard error of the estimation (see) are also given.

cluding Cycle 22, then the correlation grows ($r = 0.98$ and $see = 110$, where ‘see’ stands for standard error of the estimation). The mean and standard deviation (μ and σ in days) for the differences ‘Os’, ‘Om’ and ‘Op’, ‘Og’ are (122 and 141) and (−101 and 208), respectively. The high correlations and small differences between ‘Os’ and ‘Om’ and between ‘Op’ and ‘Og’ confirm the treatment of the LSS and the peak maxima as observables describing minima and maxima of solar activity.

We suppose that the central day of the LSS represents better the time of real minimum, interpreted according to Cameron and Schüssler (2008) as the epoch when the sum of the activities of the old and the new cycle is minimal, than the Gaussian minimum. Various definitions of the cycle minimum were considered by Harvey and White (1999), who among others took into account the monthly averages of spotless days.

3. Lengths of Intervals – Two Types of Solar Cycles

Lengths of passive and active intervals vary from cycle to cycle, as is seen in Figure 3.

Passive intervals associated with Cycles 9–15 (‘00’ = 3175 ± 192 , the mean and the standard error of the mean are given) are clearly longer than the related active intervals (‘xx’ = 998 ± 168). The mean and the standard error of the ratio are ‘xx/00’ = 0.330 ± 0.065 . In contrast to these cycles, Cycles 17–23 have short passive intervals (‘00’ = 1551 ± 76) and long active intervals (‘xx’ = 2276 ± 75) for which the mean and its standard error are ‘xx/00’ = 1.485 ± 0.079 (see Figure 4). Despite the large differences between the ratios xx/00, the additions of passive to active intervals do not differ so much for these two types of solar cycles.

To check which parameters characterizing the passive and active intervals are significantly different in both types of cycles, we applied, because of the very small number of

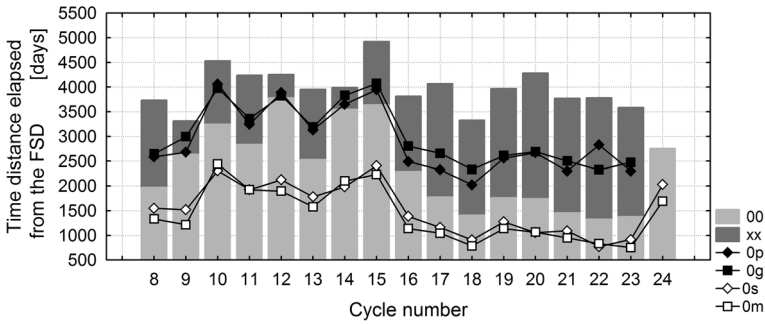


Figure 3 Cyclic variation of time distances measuring positions of the characteristic extreme points of the daily sunspot series with respect to the first spotless day (FSD) for Cycles 8–24. ‘0s’, the position of the central day of the longest spotless segment, ‘0m’, the position of the Gaussian minimum, ‘0p’, the position of the peak maximum, ‘0g’, the position of the Gaussian maximum. Vertical bars show lengths of passive ‘00’ and active ‘xx’ intervals for Cycles 8–24.

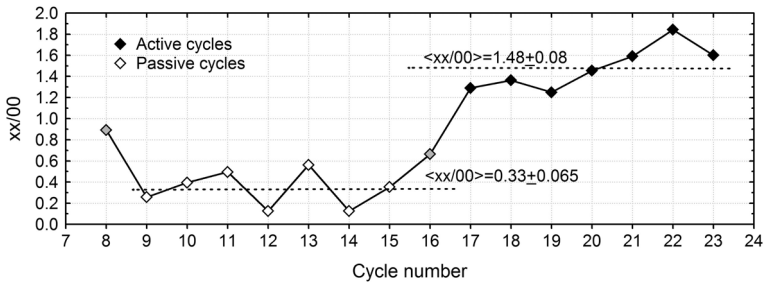


Figure 4 Scatterplot of the ratio $xx/00$ between lengths of active and passive intervals for Cycles 8–23. The mean values and the standard errors of the means are shown for the two selected types of cycles.

cases (7 cases in each type), two statistical tests: Student’s t-test and the Mann–Whitney U non-parametric test. The results are presented in Table 3.

The conclusions from a careful analysis of Table 3 are:

- i) Lengths of cycles measured from one LSS to the next one (see row 9) and the time distance from the LSS minimum to the peak maximum are the same for both types of cycles (row 8).
- ii) There are significant differences between both types of cycles in the lengths of their segments, such as ‘0s’, ‘s0’, ‘xp’, and ‘px’ (rows 2, 3, 5, 6).
- iii) The AI mean sunspot numbers of Cycles 17–23 are slightly higher than those of Cycles 9–15, but the differences are mainly in the ‘xp’ segments (rows 12, 13).
- iv) The PI mean sunspot numbers of Cycles 9–15 are significantly larger than those in the other type of cycles; this is mainly because of the relatively large sunspot numbers in their rising segments ‘s0’, along which a high variability of the sunspot numbers is also observed (rows 10, 11).
- v) The number of the spotless days, the longest spotless segments and longest segments of days with spots in a row are significantly larger in the PI of Cycles 9–15 (rows 14, 15, 16).

Table 3 Results of statistical tests calculated for various parameters of the passive and active intervals.

No.	Parameter	Cycles 9–15		Cycles 17–23		<i>p</i> -value ¹		
		Mean	SD	Mean	SD	Test F	Test t	Test U
1	Length of the PI '00'	3175.0	507.5	1551.4	200.1	0.039	0.00000	0.0006
2	Length of the PI declining segment '0s'	2009.1	306.1	1027.7	171.1	0.183	0.00001	0.0006
3	Length of the PI rising segment 's0'	1165.9	340.6	523.7	106.0	0.012	0.00046	0.0006
4	Length of the AI 'xx'	998.3	445.6	2276.3	199.0	0.071	0.00002	0.0006
5	Length of the AI rising segment 'xp'	341.4	287.8	880.1	308.9	0.868	0.00551	0.0070
6	Length of the AI declining segment 'px'	656.9	278.6	1396.1	253.7	0.826	0.00022	0.0023
7	Ratio xx/00	0.330	0.171	1.485	0.209	0.637	0.00000	0.0006
8	Time elapsed since the LSS to the day of the peak maximum 'sp'	1507.3	236.9	1403.9	332.8	0.428	0.516	0.383
9	Time distance between two subsequent LSS segments 'ss'	4154.3	216.0	3951.6	422.0	0.128	0.280	0.209
10	Mean sunspot number of the PI	30.86	6.82	22.07	4.95	0.455	0.01729	0.0379
11	Mean sunspot number of 's0' segment in the PI	30.39	11.29	18.13	2.87	0.004	0.01656	0.0262
12	Mean sunspot number of the AI	85.64	23.20	106.15	20.77	0.795	0.10684	0.0973
13	Mean sunspot number of 'xp' segment in the AI	82.37	14.26	105.48	27.56	0.134	0.07239	0.0728
14	Number of spotless days in the PI	740.6	268.9	337.7	123.2	0.079	0.00362	0.0070
15	Length of the LSS	49.86	24.84	29.14	9.60	0.036	0.062	0.0728
16	Length of the longest segment of days with spot in a row in the PI	373.1	131.6	191.9	121.5	0.851	0.02011	0.0262

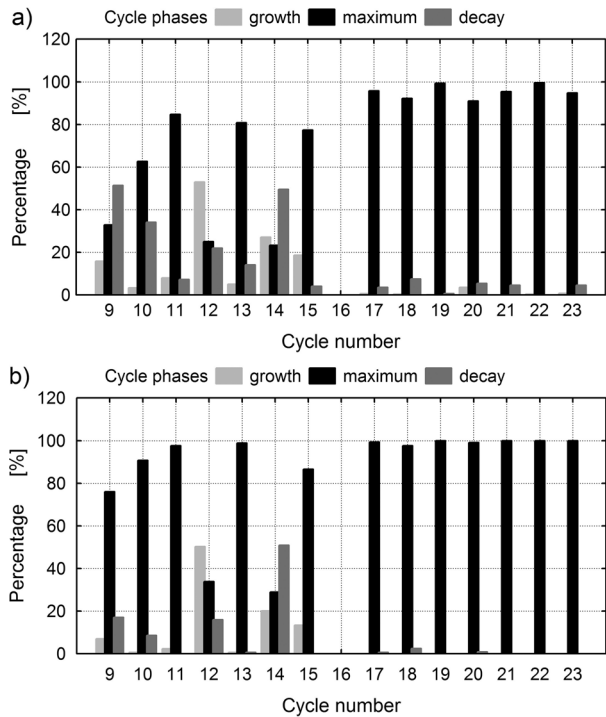
¹ *p*-value, the probability of the test statistic used for verifying the null hypothesis of tests: Test F, the F-test of equality of variances, Test t, the Student's t-test for the comparison of two means, Test U, the Mann-Whitney U non-parametric test for comparing two samples.

Large and statistically significant differences between various parameters of intervals associated with the two types of solar cycles lead us to assume that the spacing of days with small and large sunspot numbers are different. For Cycles 9–15, the probability to find a day with a relatively large sunspot number outside of the active intervals is higher than in cycles of the other type (compare Figure 1(a) with Figure 1(b) and Figure 5). We think that this division is not random but reflects some physical reason, which would explain the observed features of the pair PI-AI in these groups. Further in this article we call Cycles 9–15 the passive cycles and Cycles 17–23 the active ones (see Figure 4).

4. Amplitudes of Passive and Active Cycles

Active and passive cycles differ largely not only in the previously discussed interval lengths, but also in other features. Besides the lengths, the amplitude is the second key characteristic of a cycle. We distinguish four various measures of a cycle amplitude which can be specified for any defined time segment ('ts'): the peak amplitude RPTs, the highest sunspot number during 'ts', the mean amplitude RMts, the mean sunspot number calculated from days in the 'ts', the Gaussian maximum RGts, the maximal sunspot number in the 'ts' after smoothing

Figure 5 Distribution of the days with spots in the three phases of a solar cycle: ‘growth’, the time interval from the longest spotless segment (LSS) minimum to the last spotless day (LSD), ‘maximum’, the time interval between the LSD and the first spotless day (FSD) comprising the peak maximum, ‘decay’, the time interval between the FSD and the next LSS minimum. (a) Days with the spot number greater than 0.25 of the peak maximum. (b) Days with the spot number greater than 0.5 of the peak maximum.



the ISN time series using the 810-day Gaussian filter, the integrated amplitude RITs, the sum of daily sunspot numbers in the ‘ts’. We examine the following time segments: the passive interval ‘00’, the declining segment of the passive interval ‘0s’, the rising segment of the passive interval ‘s0’, the active interval ‘xx’, the rising segment of the active interval ‘xp’ (from the beginning of the active interval to the day of peak maximum), and the declining segment of the active interval ‘px’. Figure 6 shows the peak amplitudes which are observable values. There are three peak amplitudes linked with each active interval and two linked with each passive interval. This is a consequence of the clear division of each active and passive interval into two segments.

For the active interval, the day of the peak maximum is used as the split point, while for the passive interval, the central day of the LSS fulfills this role. The peak maxima in both segments of the passive interval are simple to define but for the active interval an additional rule is that the day corresponding to the maximum in each segment has to belong to a different solar rotation from the day of the split point.

For the active cycles the following characteristics can be noticed.

- All the three active interval peak amplitudes are apparently higher than peaks observed during passive intervals. Student’s t-test gives the p -values (see the footnote in Table 3) smaller than 0.0006 for all the possible pairs of AI peak amplitudes *versus* PI peaks. Furthermore, we find that the non-parametric Wilcoxon T test (a signed-rank paired difference test) confirms these differences by giving a p -value of 0.018 for all the pairs.
- In Figure 6, the peaks of the PI declining segments of active cycles (red circles) are typically higher than the peaks of the rising segments (red triangles). The non-parametric Wilcoxon T test gives a p -value equal to 0.028.

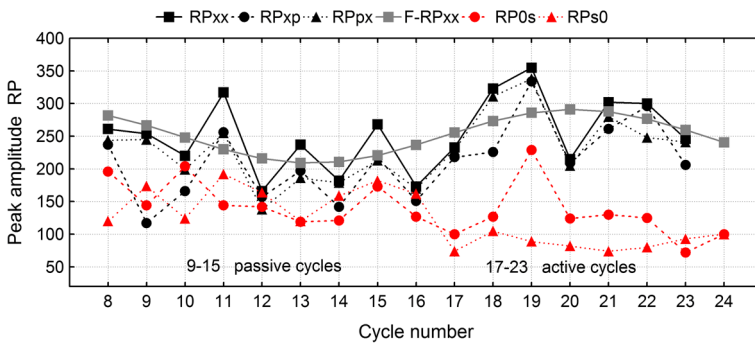


Figure 6 The scatterplots of the peak amplitude (RP) for the following time segments: the active interval ‘xx’ (RPxx), the rising segment of the active interval ‘xp’ (RPxp), the declining segment of the active interval ‘px’ (RPpx), the declining segment of the passive interval ‘0s’ (RP0s), the rising segment of the passive interval ‘s0’ (RPs0). The best sinusoidal fit (F-RPxx) for the active interval peak amplitudes is also shown. The black color is for active intervals and the red one for passive intervals.

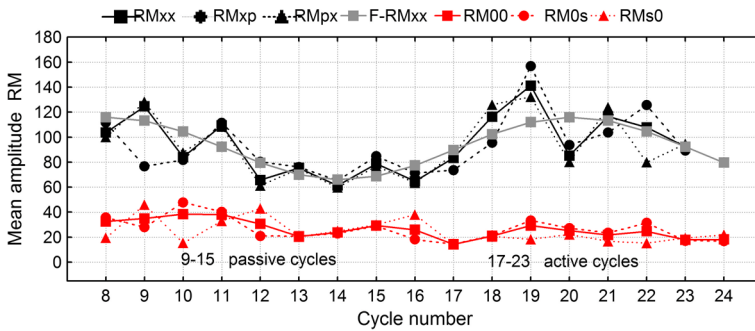


Figure 7 Similar to Figure 6, but in this case the scatterplots of the mean amplitude (RM) are shown. RM00 stands for the mean amplitude of the passive interval. The best sinusoidal fit (F-RMxx) for the active interval mean amplitudes is also shown.

- The peaks of PI rising segments of active cycles are significantly lower than the same one in the passive cycles. Student’s t-test gives a p -value equal to 0.000027 while p -value of the Mann–Whitney U non-parametric test is 0.00058.

The differences among peak amplitudes of the active and passive intervals for the passive cycles are still evident, but peaks of the AI rising segments (black circles) are not significantly higher than those characterizing the passive segments. Figures 7 to 9 are similar to Figure 6 but depict the other defined amplitudes.

In Figure 7, the curves of the mean amplitudes support the same results we infer from the curves in Figure 6. The statistical significance of the differences between the mean amplitudes of the active and passive intervals for all the cycles is evident. Results of the comparison between the mean amplitudes of the passive and active cycles calculated separately for the passive and active intervals are given in Table 3 (row 10 and 12).

Both peak and mean amplitudes of the active intervals (except for the even-odd cycle pair 22–23 and, probably, 8–9) follow the Gnevyshev–Ohl rule, which states that in consecutive odd–even cycle pairs the odd cycle tends to be the stronger (Gnevyshev and Ohl, 1948; Kopecky, 1950). Also the curves of the Gaussian maximum amplitude (RGxx in Figure 8)

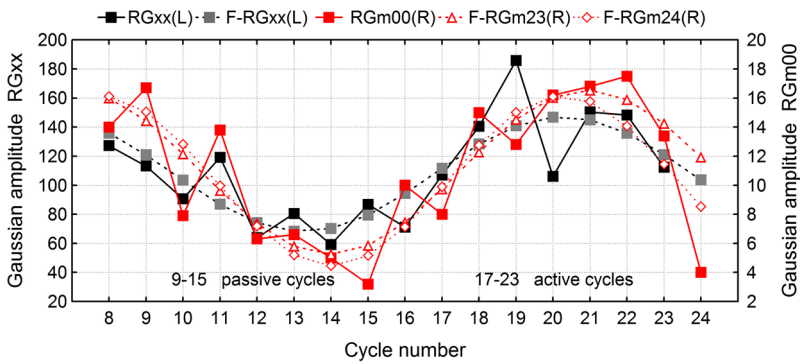


Figure 8 Scatterplot of the AI Gaussian maximum (RGxx, black) and PI Gaussian minimum (RGm00, red) amplitude. The best sinusoidal fit (F-RGxx) for the Gaussian maximum amplitude and the two best sinusoidal fits (with F-RGm24 and without F-RGm23 data for the PI 24) for the Gaussian minimum are shown.

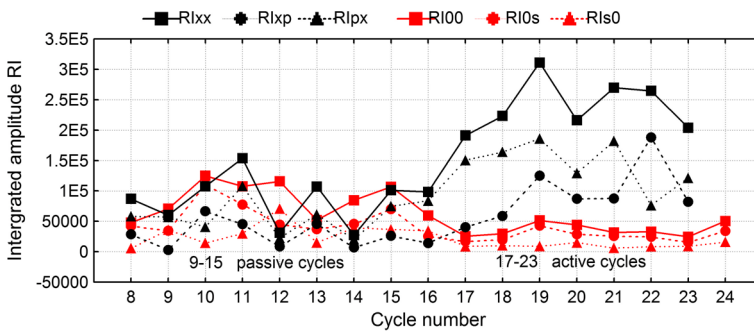


Figure 9 Similar to Figure 7, but in this case scatterplots of the integrated amplitude (RI) are shown.

and the AI integrated amplitude (RIxx in Figure 9) confirm this rule. The basic pattern of the curves in Figure 9 agrees with that in Figure 6.

The scatterplots of the AI peak, the mean and Gaussian amplitudes, and the PI Gaussian minimum amplitude suggest that these parameters can be fitted by sinusoids. The best fitted sinusoids, all in the form $y = a \cdot \sin(2\pi \cdot (n - 7)/T + \Phi) + b$ (n is the cycle number, and the other parameters are described in Table 4) are drawn in the corresponding figures.

All the best-fitted sinusoids indicate a period of about 14 solar 11-year cycles, which can be associated with the Gleissberg-cycle period (Gleissberg, 1939; Hathaway, Wilson, and Reichmann, 1999; Ogurtsov *et al.*, 2002).

5. The Relations Between the Time Distances and the Amplitudes

5.1. The Relations Between the Amplitude and the Period of Activity

The first attempt to connect the amplitude of a cycle maximum with a selected time distance was made by Wolf (1861) who noticed that “greater activity on the Sun goes with shorter periods”. This relationship is clearly seen especially when the integrated amplitude RIxx

Table 4 Parameters of the sinusoids ($Amplitude = a \cdot \sin(2\pi \cdot (n - 7)/T + \Phi) + b$, where n stands for the cycle number) that best fit the curves in Figures 6 to 8. R^2 (the coefficient of the determination) indicates how well data points fit a curve.

Amplitude	Symbol	a	T , the period	Φ	b	R^2
RPxx	F-RPxx in Figure 6	41 ± 20	13.6 ± 2.7	1.8 ± 0.9	250 ± 14	0.27
RMxx	F-RMxx in Figure 7	25 ± 6	12.0 ± 1.2	1.0 ± 0.6	91 ± 5	0.57
RGxx	F-RGxx in Figure 8	40 ± 8	14.0 ± 1.3	1.9 ± 0.4	108 ± 6	0.65
RGm00	F-RGm23 in Figure 8	5.6 ± 0.9	13.9 ± 1.2	1.6 ± 0.4	11 ± 0.7	0.77
RGm00	F-RGm24 in Figure 8	5.8 ± 1.0	12.5 ± 0.9	1.2 ± 0.4	10 ± 0.7	0.71
RGxx/RPxx	in Figure 8 in ZN ¹	0.086 ± 0.008	14.0 ± 0.6	1.9 ± 0.2	0.42 ± 0.006	0.90

¹ Zięba and Nieckarz (2012).

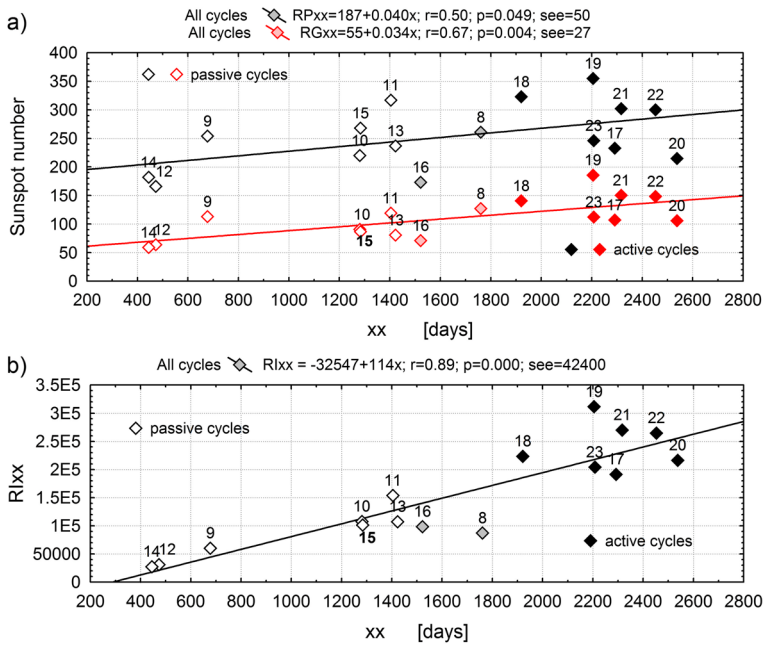


Figure 10 (a) Scatterplot of the peak (RPxx) and the Gaussian maximum (RGxx) versus lengths 'xx' for the indicated active intervals. (b) Scatterplot of the integrated amplitude (RIXx) versus 'xx'. The equation of the best linear fit and statistical parameters r , p , and the standard error of the estimation (see) are also given.

is taken as the measure of the solar activity. Figure 10 depicts the scatterplots of the peak maximum (RPxx), the Gaussian maximum (RGxx), and the integrated amplitude versus the active interval length ('xx').

Although these relationships have not directly a predictive value, 'xx' must be known from other relationships, they indicate a clear separation between passive and active cycles. The scatterplots in Figures 10(a) and (b) suggest high correlations among the three considered measures of the AI amplitude. The highest correlation coefficient, which equals 0.90, is between the peak (RPxx) and the Gaussian maximum (RGxx) (Figure 11).

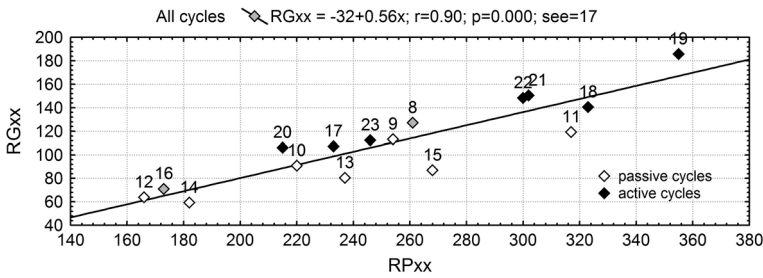


Figure 11 Scatterplot of the Gaussian maximum (RGxx) versus the peak maximum (RPxx) for the indicated AI. The equation of the best linear fit and statistical parameters r , p , and the standard error of the estimation (see) are also given.

5.2. Waldmeier Effect

The Waldmeier Effect (Waldmeier, 1935, 1939) is one of the widely quoted relationships in which the rise time elapsed between minimum and maximum of a cycle is inversely correlated with the cycle amplitude. The effect was analyzed using various monthly averages smoothed data sets such as: international (Wolf) and group sunspot numbers (Hathaway, Wilson, and Reichmann, 2002), Wolf sunspot numbers and sunspot area (Dikpati, Gilman, and de Toma, 2008), Wolf sunspot numbers, group sunspot numbers, sunspot area and 10.7 cm radio flux (Karak and Choudhuri, 2011). Among the time distances defined using the LSS location, the time distances ‘s0’ and ‘sp’ are the closest to the most commonly used definition of the rise time when the cycle maximum has occurred. The correlation coefficients between ‘sp’ and the discussed amplitudes RPxx, RGxx and RIxx are not significant (they are about -0.23), while those between ‘s0’ and these amplitudes are -0.62 , -0.76 , and -0.79 , respectively. All these values are significant with p -values smaller than 0.011.

Beside the study of the classical Waldmeier effect, some authors have tried to find correlations showing that stronger cycles tend to rise faster (Lantos, 2000; Cameron and Schüssler, 2008; Kane, 2008; Podladchikova, Lefebvre, and van der Linden, 2008; Karak and Choudhuri, 2011). There are no simple observables to measure the growth and decay rates of solar activity. Various authors proposed different approaches to define a parameter measuring a growth rate of solar activity. All these authors used monthly averages smoothed data, but took differently defined time distance values (Lantos, 2000; Karak and Choudhuri, 2011) or sunspot numbers difference (Cameron and Schüssler, 2008) between two separated months selected during the cycle’s ascending phase for their growth rate definition. Because many of the above-mentioned articles show that growth and decay rates can be treated as a precursor quantity, we examine for this purpose two values, RPOs/Os and RPs0/s0, formed by such observables as the segments ‘s0’ and ‘s0’ as well as the maximal sunspot number in these segments RPOs and RPs0. We call these ratios declining and rising indices.

Figures 13 show the best linear relations for the amplitudes versus RPOs/Os while Figures 14 correspond to the same amplitudes versus RPs0/s0. Comparing the curves presented in both of these figures, we can see that the scatter of points representing the passive cycles in Figures 13 distort the relations. Similarly, the scatter of points representing the active cycles in Figures 14 decrease the correlations. Scatterplots drawn separately for the passive and active cycles are depicted in Figure 15. The relations present in Figure 12 can be seen as an equivalent of Waldmeier effect WE1, while those in Figure 14 can be seen as the Wald-

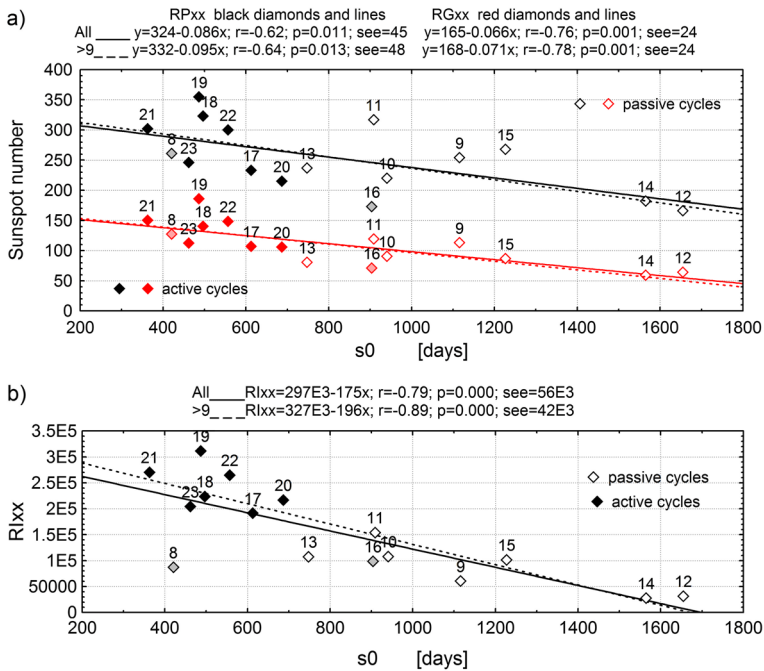


Figure 12 (a) Scatterplot of the peak (RPxx) and the Gaussian maximum (RGxx), and (b) scatterplot of the integrated amplitude (RIxx) versus lengths of the rising segment of the related passive intervals ‘s0’ for the indicated AI. The equation of the best linear fit and statistical parameters r , p , and the standard error of the estimation (see) are also given. ‘All’ denotes Cycles 8–23, while ‘> 9’ denotes Cycles 10–23.

meier effect WE2, in accordance with the distinction introduced by Karak and Choudhuri (2011).

Although both of the specified types of cycles are small samples, the correlations between the peak maximum and the RP_0/s_0 for the passive cycles and between RPO_0/s_0 for the active ones are high and statistically significant. Taking into account both of these indices and the other observables describing passive intervals, we have constructed, separately for the passive and active cycles, the best multiple-linear regression models for the maximal sunspot number RPxx and RGxx of the studied cycles. In Table 5, we present the obtained coefficients of the models together with the statistical significance of the estimated parameters and R^2 value, which checks the goodness of the fit.

6. Predictions for Cycle 24

In this section we address the prediction of the timings and the amplitude of the ongoing sunspot active interval for Cycle 24, using relations based on the description of the sunspot time series as a sequence of non-overlapping segments called passive and active intervals. Some relations inferred from the location of LSS with respect to the occurrences of the FSD and the former sunspot maximum were discussed in Zięba and Nieckarz (2012) for a prediction of the peak and the Gaussian-smoothed maximum sunspot number for the present cycle.

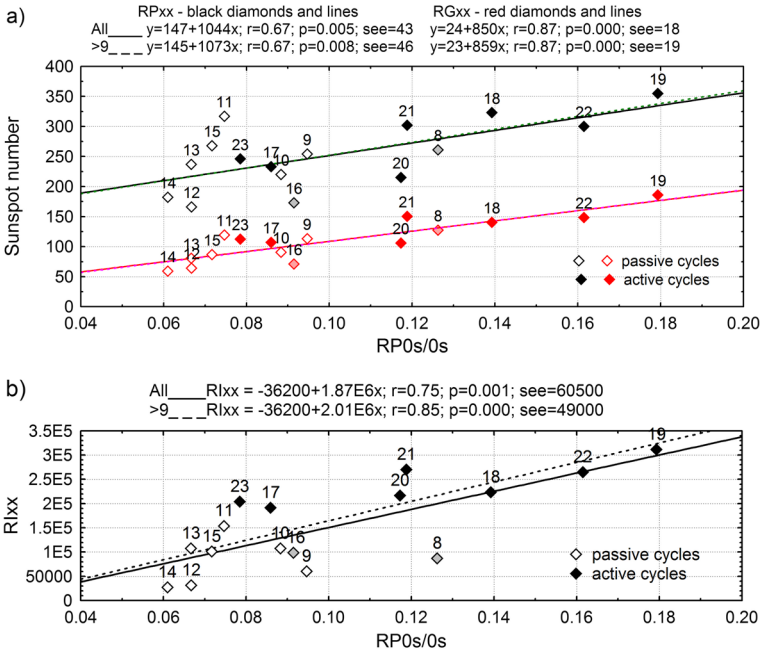


Figure 13 Similar to Figures 12(a) and (b), but in this case the scatterplots correspond to the amplitudes versus RPOs/0s.

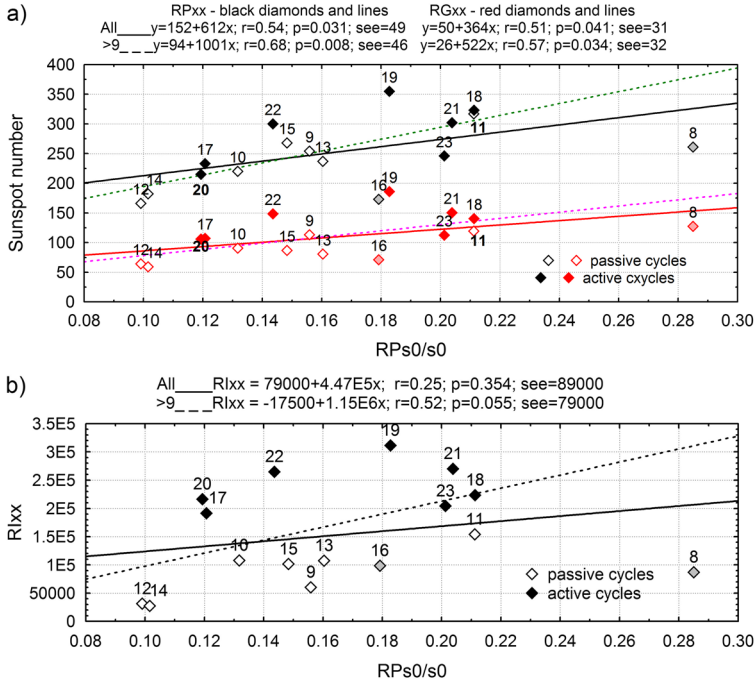
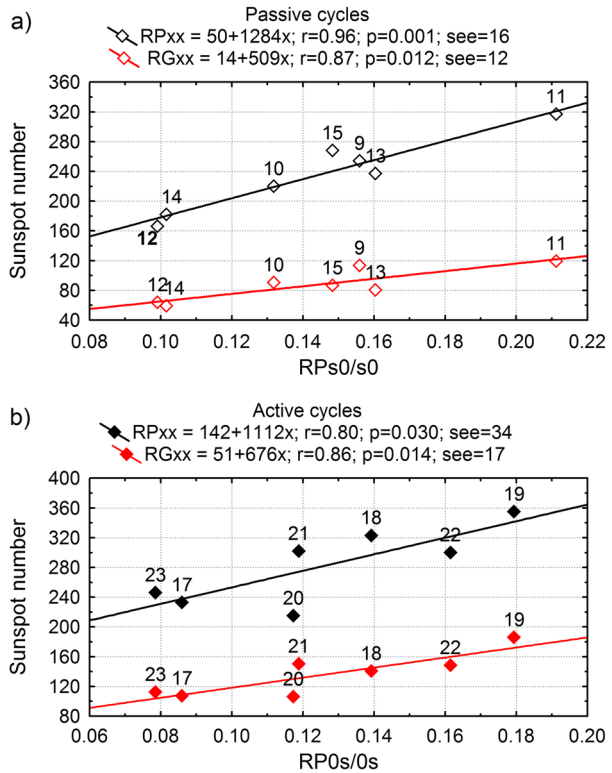


Figure 14 Similar to Figures 13(a) and (b), but in this case the scatterplots correspond to the amplitudes versus RPs0/s0.

Figure 15 Scatterplots of the peak and the Gaussian maximum amplitudes drawn for the passive (a) and active (b) cycles *versus* RP_s0/s_0 and $RPO_s/0_s$, respectively.



To assess the length of the ongoing active interval we have examined how the PI lengths ‘00’, ‘0s’ and ‘s0’ affected the length ‘xx’ of the subsequent active interval. The highest correlation coefficient was found between ‘xx’ and ‘s0’. Figure 16 presents this relation and indicates a clear concentration of active cycles near the coordinates (524, 2276). It is evident, from the curves for the passive and active cycles in Figure 17, that the lengths of the active cycles do not correlate with the ‘s0’ lengths, while the lengths of the passive cycles do.

The position of the peak maximum can also be predicted from the relations between the time distance ‘Op’ and the PI lengths ‘00’ as well as ‘0s’ (Figure 18). The correlations of these parameters with the position of the Gaussian maximum ‘0g’ are higher than those with ‘Op’ and are equal to 0.97 and 0.96, respectively.

Assuming that the ongoing Cycle 24 is a passive one, we calculated (Table 6) the peak and Gaussian maxima and other parameters for this cycle, using the models presented in Table 5 and some other relations given above.

The number of days, which elapsed from the last spotless day of the PI of Cycle 24, is 809 days counted from 31 October 2013 (the day on which this article was submitted). According to the relation presented in Figure 17, we assume that the end of the maximum phase of Cycle 24 (*i.e.* the active interval) can occur in the second half of 2015. The daily maximal ISN was 136 on 21 October 2011, but on 16 May 2013 this number was 135. Our predictions for the day of the peak maximum do not exclude that it can still happen, but the maximum value of the sunspot number is smaller than the one predicted by us (198) up to now. Our prediction for the Gaussian maximum is that it will happen around 100 days after the peak maximum.

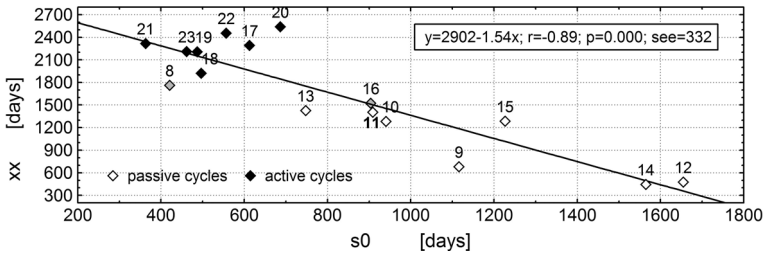


Figure 16 Scatterplot of the active interval lengths ‘xx’ versus lengths of the PI rising segments ‘s0’. The equation of the best linear fit and statistical parameters r , p , and the standard error of the estimation (see) are also given.

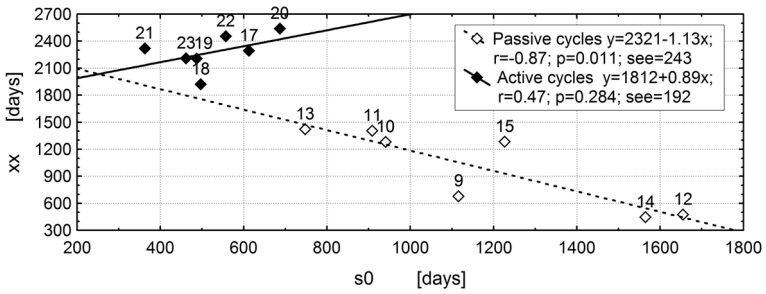


Figure 17 Similar to Figure 16, but separating the passive and active cycles.

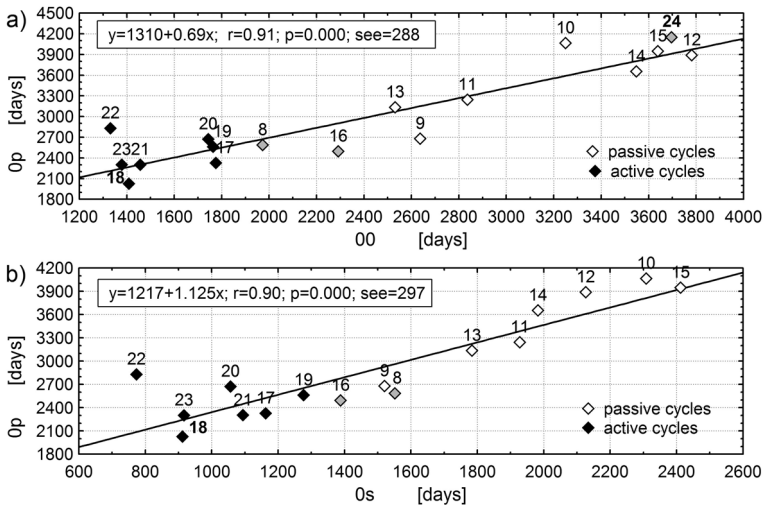


Figure 18 In (a) the position of the peak maximum with respect to the FSD of the passive interval ‘Op’ versus the length of the PI ‘00’ and in (b) versus the length of the PI declining segment ‘0s’. The equation of the best linear fit and statistical parameters r , p , and the standard error of the estimation (see) are also given.

Table 5 The parameters of the multi-linear regression models for the prediction of the maximal peak (RPxx) and Gaussian amplitude (RGxx) of the studied passive or active cycles using the following predictors (variables): RP0s/0s, the declining index, RPs0/s0, the rising index, nlss, the number of the spotless days in the LSS, n00, the number of the spotless days in the passive interval.

Passive cycle					
Model: $RP_{xx} = a + b_1 \cdot RP0s/0s + b_2 \cdot RPs0/s0 + b_3 \cdot nlss$					Analysis of variance for
Variable	Coefficient	Value	¹ Std. Error	² <i>p</i> -value	³ Regression
	<i>a</i>	-50.306	24.9104	0.13672	SSM = 15834.29 SSE = 138.57 <i>F</i> = 114.27 <i>p</i> -value = 0.00137 <i>R</i> ² = 0.9956 Adjusted <i>R</i> ² = 0.9826 see = 6.8
RP0s/0s	b1	729.391	254.7788	0.06443	
RPs0/s0	b2	1380.260	79.6949	0.00042	
nlss	b3	0.637	0.1316	0.01685	
Model: $RG_{xx} = a + b_1 \cdot RP0s/0s + b_2 \cdot RPs0/s0$					Analysis of variance for
Variable	Coefficient	Value	Std. Error	<i>p</i> -value	Regression
	<i>a</i>	-41.096	12.4554	0.02995	SSM = 2993.77 SSE = 89.04 <i>F</i> = 67.24 <i>p</i> -value = 0.00083 <i>R</i> ² = 0.9711 Adjusted <i>R</i> ² = 0.95667 see = 4.7
RP0s/0s	b1	909.152	164.3010	0.00521	
RPs0/s0	b2	421.323	52.4448	0.0013	
Active cycle					
Model: $RP_{xx} = a + b_1 \cdot RP0s/0s + b_2 \cdot RPs0/s0 + b_3 \cdot n00$					Analysis of variance for
Variable	Coefficient	Value	Std. Error	<i>p</i> -value	Regression
	<i>a</i>	-22.716	27.4782	0.46902	SSM = 15634.5 SSE = 285.5 <i>F</i> = 54.75 <i>p</i> -value = 0.004056 <i>R</i> ² = 0.9910 Adjusted <i>R</i> ² = 0.9641 see = 9.8
RP0s/0s	b1	1074.876	108.6869	0.00220	
RPs0/s0	b2	771.194	103.9258	0.00506	
n00	b3	0.116	0.0340	0.04216	
Model: $RG_{xx} = a + b_1 \cdot RP0s/0s + b_2 \cdot RPs0/s0 + b_3 \cdot n00$					Analysis of variance for
Variable	Coefficient	Value	Std. Error	<i>p</i> -value	Regression
	<i>a</i>	-25.040	30.1489	0.46714	SSM = 4807.0 SSE = 343.7 <i>F</i> = 13.98 <i>p</i> -value = 0.02868 <i>R</i> ² = 0.9333 Adjusted <i>R</i> ² = 0.8665 see = 10.7
RP0s/0s	b1	669.175	119.2504	0.01119	
RPs0/s0	b2	321.174	114.0266	0.06692	
n00	b3	0.0662	0.0373	0.17409	

¹ Std. Error, estimates how much a coefficient is likely to vary, similar to the standard error of the mean (sem).

² *p*-value the probability of a test statistic used for verifying the null hypothesis.

³ SSM, the model sum of squares, it is the sum of squared deviations of the model predicted values from the mean of the observed values, SSE, residuals sum of squares, *F*, *F*-test statistic, used in testing the model validation, *R*², the coefficient of determination, indicates how well data points fits a statistical model. An *R*² of 1 indicates that the model perfectly fits the data, Adjusted *R*² is a modification of *R*² that adjusts for the number of input variable in a model relative to the number of data points, ‘see’ is the standard error of the estimation.

7. Summary and Discussion

Taking into account spotless days, we have represented the ISN time series as the sequence of precisely defined consecutive time intervals, called passive and active intervals, according

Table 6 Some predictions for the AI in Cycle 24 derived from the relations found from previous cycles.

Variables		r	Fig.	Equation $y = a + bx$		See	y	Prediction for the AI of Cycle 24
x	y			a	b			
$s_0 = 727$	xx	-0.89	17	2321	-1.13	243	1499	¹ FSD 72217 Sep 2015
$0_0 = 2757$	0p	0.91	18a	1310	0.69	248	3212	² DPx 71174 Nov 2012
	0g	0.97	-	1414	0.69	148	3316	² DGx 71278 Feb 2013
$0_s = 2029$	0p	0.90	18b	1218	1.12	297	3490	DPx 71452 Aug 2013
	0g	0.96	-	1327	1.12	170	3599	DGx 71561 Dec 2013
$RP_0s/0_s = 0.0527$	RPxx	R^2 0.983	See Table 5 for the parameters of the linear regression.			7	198	95 % CI 175–222
$RP_s0/s_0 = 0.1375$ nlss = 32	RGxx	R^2 0.956				5	64	54–76

¹ FSD, the first spotless day of the PI of Cycle 25 at the end of the AI of Cycle 24.

² DPx, DGx, the day of the peak and Gaussian maximum, respectively.

to whether they contain minimal or maximal daily sunspot numbers. Active intervals correspond to a phase of maximal sunspot numbers (both the peak and the Gaussian maximum are inside an AI), but passive intervals are extended beyond a classically understood minimum phase of the solar cycle and include the declining phase of the previous maximum. The properties of each passive interval, such as characteristic lengths, numbers of spotless days, declining, and rising indices are predictors of the length and amplitudes of the approaching active interval.

We have found clear differences between properties of two types of solar cycles (see Table 3) referred to as the passive (Cycles 9–15) and active (Cycles 17–23) cycles. Each group contains seven cycles in a row. According to the Hathaway division of cycles into small, medium and large (Hathaway, 2010, 2011), the passive cycles are small and medium ones, while the active cycles are large and medium. The distribution of days with spots having a relatively high sunspot number is different in the both types of cycles (see Figure 5). All the three discussed cycle amplitudes (the peak, the Gaussian, and the integrated one) show a variation with time that can be fitted using sinusoidal functions. The periods of these functions (see Table 4) change from 12 to 14 solar 11-year periods. These facts indicate that the occurrence of passive and active cycles can be connected with a higher mode of the Gleisberg cycle (Gleissberg, 1939; Ogurtsov *et al.*, 2002).

Analyzing the influence of different properties of the passive intervals on the length and amplitudes of the related active intervals we have shown that solar activity in the PI declining-segment (a decay phase of the previous cycle) has a greater impact on the strength of the approaching maximum in the case of the active cycles, while activity in the PI rising-segments in the case of the passive cycles. To circumscribe solar activity in the PI segments we have introduced indices defined as a ratio of the maximal sunspot number recorded during the declining or the rising PI segment to the length of this segment ($RP_0s/0_s$ and RP_s0/s_0 , respectively). We have found multi-linear relations (see Table 5) predicting the strength of the approaching maximum using the introduced indices. The linear version of these models

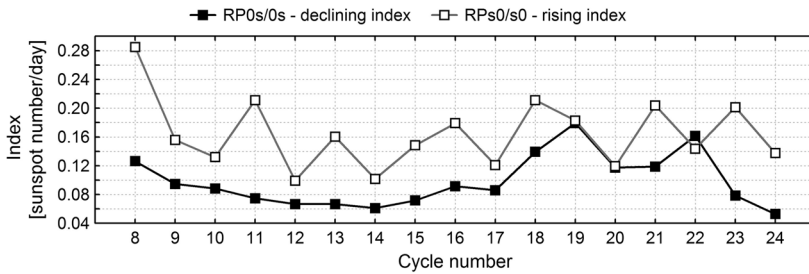


Figure 19 Values of the declining and rising index calculated for the subsequent passive intervals (epochs of solar minimum previous to the maxima indicated by the cycle number).

(see Figure 15) can be considered as the Waldmeier effect WE2, while the relation seen in Figure 12 can be seen as the Waldmeier effect WE1, in accordance with the distinction introduced by Karak and Choudhuri (Karak and Choudhuri, 2011).

The variations of these indices, which are the main predictors of the multi-linear models, with solar cycles are presented in Figure 19. The declining index (RP0s/0s) is small and practically constant for the passive cycles and rises to a statistically significantly higher values for the active cycles. The opposite is observed for the rising index (RP0s/0s). Its values fluctuate around 0.16 in both groups.

The main questions resulting from our analysis based on the daily sunspot time series can be formulated as follows:

- i) What is the cause of the apparent difference between passive and active cycles? We can answer that it can be either the specific cycle phase division based on the spotless days or that there is a key physical reason that underlies the different observed distribution of days with a relatively high sunspot number for this group of cycles. The fact that the passive and active cycles occur in a row, and in a number which corresponds to the Gleisberg cycle, indicates a possible underlying physical cause.
- ii) The cycle overlapping effect revealed by Cameron and Schüssler (2007, 2008) can explain the high fluctuation of the sunspot numbers of the passive cycles during their passive intervals (a relatively large overlapping) as well as the marked reduction of this fluctuation in the case of the active cycles (a small overlapping). This is also confirmed by the large number of spotless days during the passive cycles because their long passive intervals lead to more days without activity even if some days have relatively large sunspot numbers.

However, we cannot say whether changes of the declining index (see Figure 19) are related only to the overlapping of cycles and the Waldmeier effect (Cameron and Schüssler, 2007), or whether they are connected also with the meridional plasma flow variations considered by Nandy, Muñoz-Jaramillo, and Martens (2011). Similarly, it is difficult to assume without further study that one of the various possible mechanisms, *i.e.* the evolution of the polar field around solar minimum, could explain the observed fluctuations of our rising index (Cameron *et al.*, 2010, 2013; Dasi-Espuig *et al.*, 2010; Jiang *et al.*, 2010; Cameron and Schüssler, 2012).

Svalgaard and Kamide (2013) have shown that the polar fields play a crucial role in the solar cycle. Because of solar-cycle N–S asymmetries, polar-field reversals do not occur at the same times in both hemispheres (Norton and Gallagher, 2010; Muñoz-Jaramillo *et al.*, 2013b, 2013a; Zhao, Landi, and Gibson, 2013), and some differences among various passive intervals may be expected. The long-term persistence of a phase leading in one of the

hemispheres (Zolotova *et al.*, 2009) can explain a repetition of some noticed properties of passive and active intervals.

The focus of this article is to analyze the daily sunspot time series using the days for which timing and sunspot number are precisely defined, and we have done so. We have, however, found some other facts and characteristics that will be the object of further analysis.

Acknowledgements We thank the anonymous referee for constructive comments and suggestions, which much improved the original version of the manuscript.

Open Access This article is distributed under the terms of the Creative Commons Attribution License which permits any use, distribution, and reproduction in any medium, provided the original author(s) and the source are credited.

References

- Cameron, R.H., Schüssler, M.: 2007, *Astrophys. J.* **659**, 801.
- Cameron, R., Schüssler, M.: 2008, *Astrophys. J.* **685**, 1291.
- Cameron, R.H., Schüssler, M.: 2012, *Astron. Astrophys.* **548**, A57.
- Cameron, R.H., Das-Espuig, M., Jiang, J., Işik, E., Schmitt, D., Schüssler, M.: 2013, *Astron. Astrophys.* **557**, A141.
- Cameron, R.H., Jiang, J., Schmitt, D., Schüssler, M.: 2010, *Astrophys. J.* **719**, 264.
- Clette, F., Berghmans, D., Vanlommel, P., Van der Linden, R.A.M., Koeckelenbergh, A., Wauters, L.: 2007, *Adv. Space Res.* **40**, 919.
- Dasi-Espuig, M., Solanki, S.K., Krivova, N.A., Cameron, R.H., Peñuela, T.: 2010, *Astron. Astrophys.* **518**, A97.
- Dikpati, M., Gilman, P.A., de Toma, G.: 2008, *Astrophys. J.* **673**, L99.
- Gleissberg, W.: 1939, *Observatory* **62**, 158.
- Gnevyshev, M.N., Ohl, A.I.: 1948, *Astron. Zh.* **25**, 8.
- Harvey, K.L., White, O.R.: 1999, *J. Geophys. Res.* **104**, 19759.
- Hathaway, D.H.: 2010, *Living Rev. Solar Phys.* **7**, 1.
- Hathaway, D.H.: 2011, *Solar Phys.* **273**, 221.
- Hathaway, D.H., Wilson, R.M., Reichmann, E.J.: 1999, *J. Geophys. Res.* **104**, 22375.
- Hathaway, D.H., Wilson, R.M., Reichmann, E.J.: 2002, *Solar Phys.* **211**, 357.
- Jiang, J., Işik, E., Cameron, R.H., Schmitt, D., Schüssler, M.: 2010, *Astrophys. J.* **717**, 597.
- Kane, R.P.: 2008, *Solar Phys.* **248**, 203.
- Karak, B.B., Choudhuri, A.R.: 2011, *Mon. Not. Roy. Astron. Soc.* **410**, 1503.
- Kopecky, M.: 1950, *Bull. Astron. Inst. Czechoslov.* **2**, 14.
- Lantos, P.: 2000, *Solar Phys.* **196**, 221.
- McKinnon, J.A.: 1987, UAG Repots UAG-95, National Geophysical Data Center, NOAA, Boulder, CO.
- Muñoz-Jaramillo, A., Balmaceda, L.A., DeLuca, E.E.: 2013a, *Phys. Rev. Lett.* **111**, 041106.
- Muñoz-Jaramillo, A., Dasi-Espuig, M., Balmaceda, L.A., DeLuca, E.E.: 2013b, *Astrophys. J. Lett.* **767**, L25.
- Nandy, D., Muñoz-Jaramillo, A., Martens, P.C.H.: 2011, *Nature* **471**, 80.
- Norton, A.A., Gallagher, J.C.: 2010, *Solar Phys.* **261**, 193.
- Ogurtsov, M.G., Nagovitsyn, Y.A., Kocharov, G.E., Jungner, H.: 2002, *Solar Phys.* **211**, 371.
- Podladchikova, T., Lefebvre, B., van der Linden, R.: 2008, *J. Atmos. Solar-Terr. Phys.* **70**, 277.
- Svalgaard, L., Kamide, Y.: 2013, *Astrophys. J.* **763**, 23.
- Waldmeier, M.: 1935, *Astron. Mitt. Eidgenöss. Sternwarte Zür.* **14**(133), 105.
- Waldmeier, M.: 1939, *Astron. Mitt. Eidgenöss. Sternwarte Zür.* **14**(138), 470.
- Waldmeier, M.: 1961, *The Sunspot-Activity in the Years 1610–1960*, Schulthess, Zürich.
- Wilson, R.M.: 1995, *Solar Phys.* **152**, 197.
- Wilson, R.M.: 1998, *Solar Phys.* **182**, 217.
- Wilson, R.M., Hathaway, D.H.: 2005, NASA Technical Report, NASA/TP-2005-213608.
- Wilson, R.M., Hathaway, D.H.: 2006, NASA Technical Report, NASA/TP-2006-214601.
- Wilson, R.M., Hathaway, D.H.: 2007, NASA Technical Report, NASA/TP-2007-215134.
- Wolf, R.: 1861, *Mon. Not. Roy. Astron. Soc.* **21**, 77.
- Zhao, L., Landi, E., Gibson, S.E.: 2013, *Astrophys. J.* **773**, 157.
- Zięba, S., Masłowski, J., Michalec, A., Michałek, G., Kulak, A.: 2006, *Astrophys. J.* **653**, 1517.
- Zięba, S., Nieckarz, Z.: 2012, *Solar Phys.* **278**, 457.
- Zolotova, N.V., Ponyavin, D.I., Marwan, N., Kurths, J.: 2009, *Astron. Astrophys.* **503**, 197.